Exploring Hypoxia-Related Genes as Prognostic Indicators in Lung Adenocarcinoma

Bandar Alghamdi[1] and Sonia Rocha[2]*

[1]IKing Fahad Army Forces Hospital, cardiology and cardiac surgery center, Jeddah, Saudi Arabia.

[2]Department of Biochemistry, Cell and Systems Biology, Institute of Systems Molecular and Integrative Biology, University of Liverpool. Liverpool United Kingdom.

*correspondence to: Sonia Rocha srocha@liverpool.ac.uk

Abstract

Background: Lung adenocarcinoma (LUAD) is a leading cause of cancer-related mortality, with hypoxia contributing to tumor progression and treatment resistance. Identifying hypoxia-related biomarkers could enhance prognosis and therapeutic strategies for LUAD. **Methods:** This study aimed to identify hypoxia-related differentially expressed genes (HRDEGs) in lung adenocarcinoma (LUAD) through differential expression analysis. Functional analysis and protein-protein interaction (PPI) network construction were performed to explore the biological roles and interactions of these genes. Kaplan-Meier survival analysis, univariate Cox regression, and Lasso regression were used to identify key genes associated with survival. Multivariate Cox regression was then conducted to assess independent prognostic factors. **Results:** This analysis revealed 283 upregulated HRDEGs and 322 downregulated HRDEGs in LUAD. Functional enrichment analysis indicated that the upregulated genes were primarily involved in cancer-related and cellular signaling pathways, while downregulated genes were associated with immunity-related pathways. We further identified 201 common upregulated hub genes (including *MMP9, CDH1, HSP90AB1, SOX2, CDKN2A, SPP1, EZH2*) and 224 common downregulated hub genes (such as *IL6, TNF, IL1B, JUN, CCL2, TLR4, FOS, PTGS2*). Kaplan-Meier survival analysis, univariate Cox regression, and Lasso regression led to the identification of 17 key genes (*ADRB2, ALDH2, CAT, CCNE1, MAP3K8, DSG2, EIF6, ABCB1, PIK3R1, RAD51, SFTPD, SOD3, CLEC3B, ADAM12, EXO1, FBLN5,* and *IGF2BP3*) associated with patient survival. Finally, multivariate Cox regression analysis identified *DSG2, EIF6,* and *EXO1* as independent prognostic factors for LUAD, highlighting their potential as biomarkers for prognosis and therapeutic targets in lung cancer. **Conclusion:** In conclusion, *DSG2, EIF6,* and *EXO1* were identified as key hypoxia-related genes in lung adenocarcinoma. These genes were

found to be independent prognostic factors, highlighting their potential as biomarkers for predicting patient survival and guiding future therapeutic approaches.

Keyword: Lung Adenocarcinoma, Hypoxia-Related Differentially Expressed Genes, immunity, independent prognostic factors

Authors summary:

This study investigates the role of hypoxia-related genes in lung adenocarcinoma (LUAD), a major cause of cancer mortality. By analyzing gene expression data, this study identified 283 upregulated and 322 downregulated hypoxia-related differentially expressed genes (HRDEGs). Functional enrichment analysis revealed that the upregulated genes are largely involved in cancer progression and cell signaling, while the downregulated ones are linked to immune responses. A set of key hub genes was identified through protein-protein interaction analysis. Using survival analysis tool, 17 genes significantly associated with patient outcomes in two different patient cohorts. Among these, confirmed three genes—DSG2, EIF6, and EXO1—were confirmed as independent prognostic markers. These findings suggest that these genes may serve as valuable biomarkers for predicting survival and developing targeted therapies in LUAD, offering new avenues for improving patient management in hypoxia-driven tumors.

Introduction

Lung Adenocarcinoma and Hypoxia Lung cancer remains one of the most common and deadly cancers worldwide, with non-small cell lung cancer (NSCLC) being the dominant histological subtype (1). Lung adenocarcinoma (LUAD) is the most prevalent histological subtype of NSCLC and represents a major clinical and biological focus within this disease category due to its distinct molecular and genetic characteristics. Although advances in molecular profiling and targeted therapies have improved the management of NSCLC, the prognosis for patients with LUAD remains poor, particularly in advanced stages (2). The overall five-year survival rate for LUAD patients is low, making it essential to identify novel biomarkers for early diagnosis, prognosis, and therapeutic targeting (3). One of the critical microenvironments influencing cancer progression, metastasis, and resistance to therapy is tumor hypoxia. Hypoxia refers to the state of low oxygen availability within the tumor, often resulting from an imbalance between the rapid growth of tumor cells and the insufficient development of blood vessels to supply oxygen (4). Hypoxia is a hallmark feature of many solid tumors, including lung adenocarcinoma, and it is associated with aggressive tumor behavior, poor prognosis, and resistance to conventional therapies (5). The development of therapeutic strategies targeting hypoxic tumor cells remains an area of active research.

The Role of Hypoxia in Tumorigenesis Hypoxia plays a crucial role in driving various aspects of tumor biology, such as tumor angiogenesis, metabolic reprogramming, and epithelial-to-mesenchymal transition (EMT) (6). It activates a range of adaptive cellular responses through hypoxia-inducible factors (HIFs), primarily HIF-1α and HIF-2α. These transcription factors regulate the expression of genes that mediate critical processes such as angiogenesis (formation of new blood vessels), glycolysis, metastasis, and drug resistance (7, 8). Tumor cells exposed to

hypoxic conditions undergo metabolic shifts that favor anaerobic glycolysis, which allows them to survive and proliferate despite low oxygen availability. The HIF signaling pathway is essential for the regulation of genes involved in cellular survival, metabolism, and tumor progression (9). Among the most well-known hypoxia-regulated genes are vascular endothelial growth factor (VEGF), glucose transporter proteins (e.g., GLUT1), and matrix metalloproteinases (e.g., MMPs) (10). These genes promote tumor growth and metastasis by facilitating the adaptation of tumor cells to low-oxygen conditions. Additionally, hypoxia is implicated in the regulation of immune evasion and resistance to chemotherapies and radiation therapy, further complicating treatment strategies (11). Therefore, the identification of key hypoxia-related genes and their role in LUAD progression and prognosis is crucial for improving the clinical management of lung adenocarcinoma.

The link between hypoxia and poor prognosis in LUAD has been well established through various studies. Tumors with hypoxic regions have been shown to have a higher potential for metastasis, increased tumor aggressiveness, and reduced sensitivity to treatment (12). Patients with high expression levels of hypoxia-related genes often exhibit shorter overall survival and progression-free survival compared to those with low expression levels of these genes (13).Several studies have sought to identify specific hypoxia-related biomarkers that could serve as predictors of patient outcomes in LUAD (14). However, the heterogeneity of LUAD, coupled with the complexity of hypoxia-induced changes in gene expression, presents challenges in pinpointing specific prognostic genes. Additionally, the tumor microenvironment in LUAD is influenced by various factors, such as genetic mutations, immune responses, and stromal interactions, which may confound the impact of hypoxia on survival (15, 16).

In this context, a comprehensive analysis of hypoxia-related genes and their potential prognostic value in LUAD is crucial. Identifying genes that are consistently associated with poor prognosis, regardless of other clinical variables, will allow for the development of better prognostic models. These models could guide personalized treatment strategies, such as targeting hypoxic regions of the tumor with hypoxia-activated prodrugs or improving the efficacy of therapies through the modulation of the HIF pathway.

This study aims to systematically investigate hypoxia-related genes in LUAD and evaluate their potential prognostic significance. We used a combination of computational and statistical approaches to analyze large-scale genomic datasets. By identifying key hypoxia-associated genes, this work seeks to find independent prognostic biomarkers and provide insights into hypoxia-driven mechanisms underlying disease progression in LUAD.

Methods

Data downloading and processing

The analysis utilized two distinct datasets: the TCGA LUAD cohort and GSE18842. We downloaded the TCGA LUAD cohort form the cBioPortal (17). The TCGA LUAD cohort comprised 517 tumor samples and 59 control samples, representing lung adenocarcinoma (LUAD) patients and normal controls, respectively (https://www.cbioportal.org/study/summary?id=luad_tcga). Clinical data (https://www.cbioportal.org/study/summary?id=luad_tcga) from this cohort were incorporated for Kaplan-Meier survival analysis, univariate regression analysis, and multivariate regression analysis to investigate the relationship between gene expression and survival outcomes. For the GSE18842 dataset, which contains 46 tumor samples and 45 control samples. data normalization was performed using a log2 transformation. To account for multiple probes corresponding to individual genes, the data was averaged, resulting in a single expression value for each gene. The GSE18842 dataset is publicly available and can be accessed at https://www.ncbi.nlm.nih.gov/geo/query/acc.cgi?acc=GSE18842.

Differentially expressed genes identifications

In this study, we utilized multiple datasets to identify differentially expressed genes (DEGs) associated with tumorigenesis. To identify DEGs between tumor and normal samples, we employed the LIMMA package, applying a stringent cutoff of $|\log2FC| > 0.585$ and an adjusted p-value < 0.05. Following DEG identification, we specifically targeted hypoxia-related differentially expressed genes (HRDEGs), which were selected through a Venn diagram approach. This method allowed us to cross-reference the LUAD DEGs and further refine the set of genes related to hypoxia, thus providing a focused analysis of the genes potentially involved in the tumor microenvironment's hypoxic conditions.

Curation of hypoxia related genes and identification of hypoxia related differentially expressed genes (HRDEGs)

To curate a comprehensive list of hypoxia-related genes, we integrated data from several established resources. First, we retrieved hypoxia-related genes from Gene Set Enrichment Analysis (GSEA) (https://www.gsea-msigdb.org/gsea/index.jsp), focusing on the following gene sets: GOBPHYPOXIAINDUCIBLEFACTOR1ALPHASIGNALINGPATHWAY, GOBPINTRINSICAPOPTOTICSIGNALINGPATHWAYINRESPONSETOHYPOXIA, GOBPNEGATIVEREGULATIONOFCELLULARRESPONSETOHYPOXIA, GOBPNEGATIVEREGULATIONOFHYPOXIAINDUCEDINTRINSICAPOPTOTICSIGNALINGPATHWAY,GOBPREGULATIONOFCELLULARRESPONSETOHYPOXIA, HALLMARKHYPOXIA, and REACTOMEREGULATIONOFGENEEXPRESSIONBYHYPOXIAINDUCIBLEFACTOR. We then performed a search on OMIM (https://www.ncbi.nlm.nih.gov/omim/?term=HYPOXIA) using the term "HYPOXIA" to identify genes associated with hypoxia-related genetic disorders. Additionally, we retrieved genes from the hsa04066:HIF-1 signaling pathway in the KEGG database (https://www.genome.jp/kegg/). Finally, we obtained genes from GeneCards (https://www.genecards.org/), selecting those with a score greater than or equal to 1. After compiling the data from these sources, we performed deduplication to ensure that only unique genes were included. This resulted in a final list of 3292unique genes, which are tabulated in **Supplementary Table S1**.

Functional enrichment analysis of DEGs

We used DAVID v6.8 (https://david.ncifcrf.gov/) (18) to perform functional annotation of the identified genes. This platform allowed us to categorize the genes into various biological contexts, such as significantly enriched KEGG pathways, biological processes, cellular components, and molecular functions. These functional analyses provided valuable insights into the roles and interactions of the genes in key cellular mechanisms. To assess the statistical significance of the enrichment, we applied a false discovery rate (FDR) threshold of < 0.05, calculated using the Benjamini–Hochberg method (19), ensuring that only robust and biologically relevant findings were included.

Exploration of hub HRDEGs

We constructed Protein-Protein Interaction (PPI) networks for the differentially expressed genes (DEGs) using STRING v11.0 (https://string-db.org/) (20)). Both upregulated and downregulated genes were entered into the STRING search module to generate the interaction networks. To identify key hub genes within these networks, we utilized the cytoHubba plugin in Cytoscape (https://cytoscape.org/) (21),which ranks genes based on their interaction degree. A medium interaction score threshold of ≥ 0.40 was applied to build the PPI network, and genes with an interaction degree of ≥ 10 were selected for further analysis. This approach enabled us to focus on the most significant hub genes, highlighting those with strong interactions relevant to lung cancer.

Exploration of survival associated hub HRDEGs

We retrieved clinical data from TCGA LUAD to perform an analysis of overall survival (OS) in relation to gene expression. Patients were categorized into two groups based on their gene expression levels, either above or below the median, and survival rates between these groups

were compared. To further explore survival differences, patients were also stratified into risk groups based on their gene expression profiles. The log-rank test and Kaplan-Meier survival curves were utilized to evaluate and visualize differences in survival outcomes. For a more detailed survival analysis, we used the R package "survival" (22), performing both univariate and multivariate Cox regression analyses to assess the independent effects of genes on survival. Additionally, we applied LASSO-Cox regression via the "glmnet" package (23), incorporating 10-fold cross-validation to optimize the selection of penalty parameters and minimize the risk of overfitting. This comprehensive approach allowed us to identify significant survival-associated genes while controlling for potential biases and overfitting, ensuring robust and reliable findings.

Validation of Prognostic Signature in an Independent Cohort

To validate the prognostic relevance of the identified three-gene signature, we utilized the independent LUAD dataset GSE13213 via the SurvExpress platform (24). SurvExpress is an online tool that allows assessment of gene expression-based prognostic models across independent cohorts. The expression levels of gene signature were used to calculate a risk score for each patient, and patients were stratified into high-risk and low-risk groups based on the median risk score. Survival differences between the groups were evaluated using Kaplan-Meier survival analysis and the Log-Rank test**,** and hazard ratios (HRs) with 95% confidence intervals were computed to assess prognostic significance. Additionally, expression differences of gene signature between the risk groups were compared to confirm consistency with the primary cohort findings.

Statistical analysis and overall methodology

All statistical analyses were performed using R software (version 4.0.1). Differentially expressed genes (DEGs) were identified using a cutoff threshold of |log□ fold change (log□FC)|> 0.585 and an adjusted p-value < 0.05. Multiple testing correction was conducted using the Benjamini–Hochberg false discovery rate (FDR) method, with an FDR threshold of < 0.05 applied to control for false positives (19). The overall methodology provided in the Figure 1.

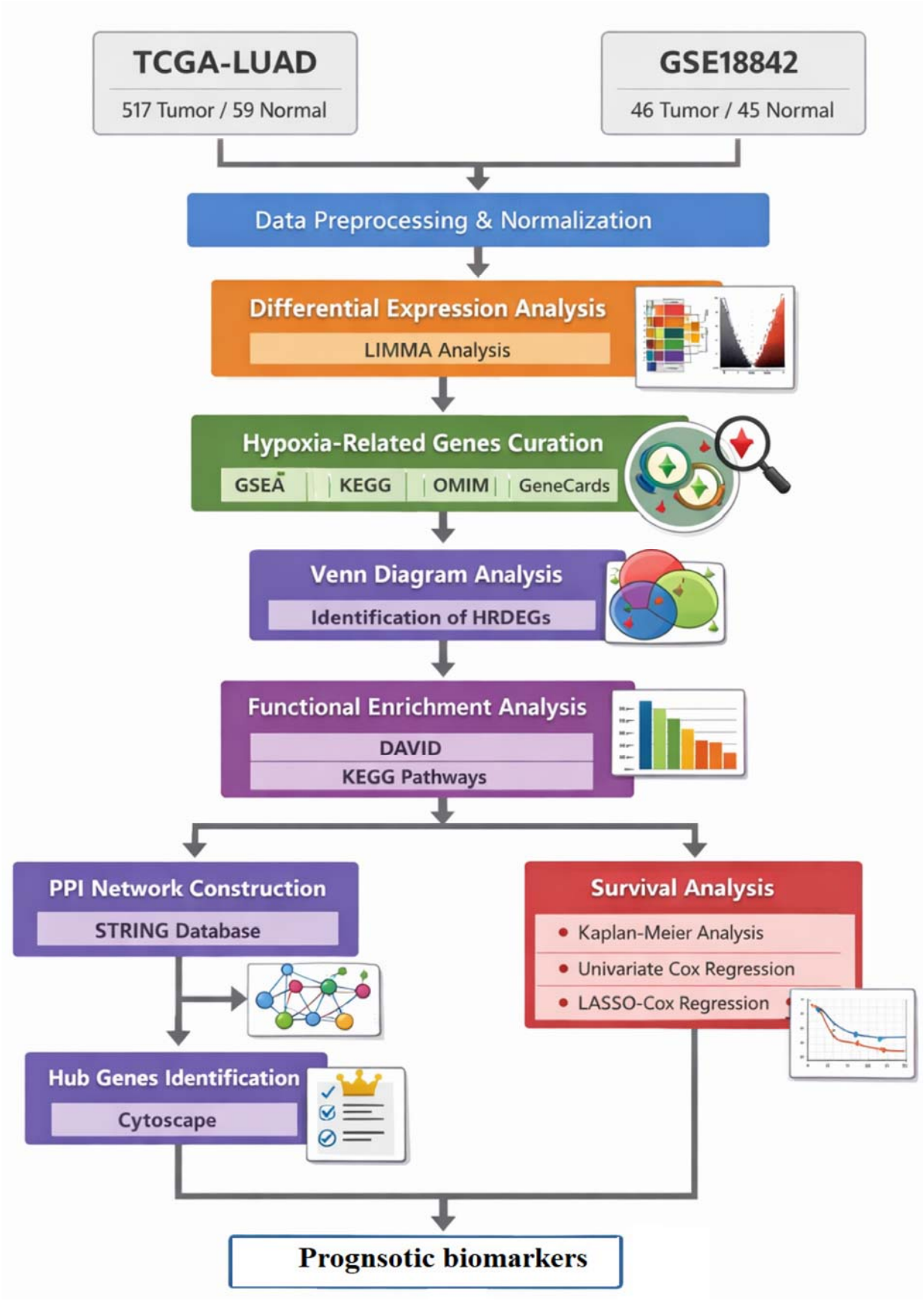
TCGA-LUAD
517 Tumor / 59 Normal
GSE18842
46 Tumor / 45 Normal
Data Preprocessing & Normalization
Differential Expression Analysis
LIMMA Analysis
Hypoxia-Related Genes Curation
GSEA
KEGG
OMIM
GeneCards
Venn Diagram Analysis
Identification of HRDEGs
Functional Enrichment Analysis
DAVID
KEGG Pathways
PPI Network Construction
STRING Database
Survival Analysis
Kaplan-Meier Analysis
Univariate Cox Regression
LASSO-Cox Regression
Hub Genes Identification
Cytoscape
Prognsotic biomarkers

208

Figure 1. The overall methodology of the study.

Result and discussion

Identification of hypoxia related differentially expressed genes (HRDEGs) in Lung adenocarcinoma

We explored differentially expressed genes (DEGs) in the TCGA LUAD cohort (**Supplementary Table S2**) and identified additional DEGs from the GSE18842 dataset (**Supplementary Table S3**). Volcano plots depicting the results of both analyses are shown in **Figure 2A** and **Figure 2B**, respectively. These plots provide a visual representation of the relationship between fold changes (logFC) and adjusted p-values, helping to identify genes with significant differential expression in lung adenocarcinoma (LUAD). Next, we compared the identified DEGs with hypoxia-related genes to determine the hypoxia-related differentially expressed genes (HRDEGs). This comparison revealed a total of 283 upregulated HRDEGs and 322 downregulated HRDEGs in LUAD, which are displayed in **Figure 2C-D** and detailed in **Supplementary Table S4**. These findings indicate that specific hypoxia-related genes are significantly altered in LUAD, providing potential insights into the molecular mechanisms underlying the disease. The top ten upregulated and downregulated HRDEGs are listed in Table 1. Among the top upregulated HRDEGs are *CYP24A1*, *CA9*, *MMP13*, *SPP1*, *COL10A1*, *MMP1*, *EEF1A2*, *GREM1*, *PITX1*, and *MMP12*. These genes are associated with various biological processes such as cell metabolism, matrix remodeling, and tumor progression. On the other hand, the top downregulated HRDEGs include *SFTPC*, *SLC6A4*, *AGER*, *FABP4*, *SCGB1A1*, *VEGFD*, *HBB*, *SFTPA2*, *AQP4*, and *CLEC3B*, which are involved in processes like lung surfactant production, cell signaling, and vasculature maintenance.

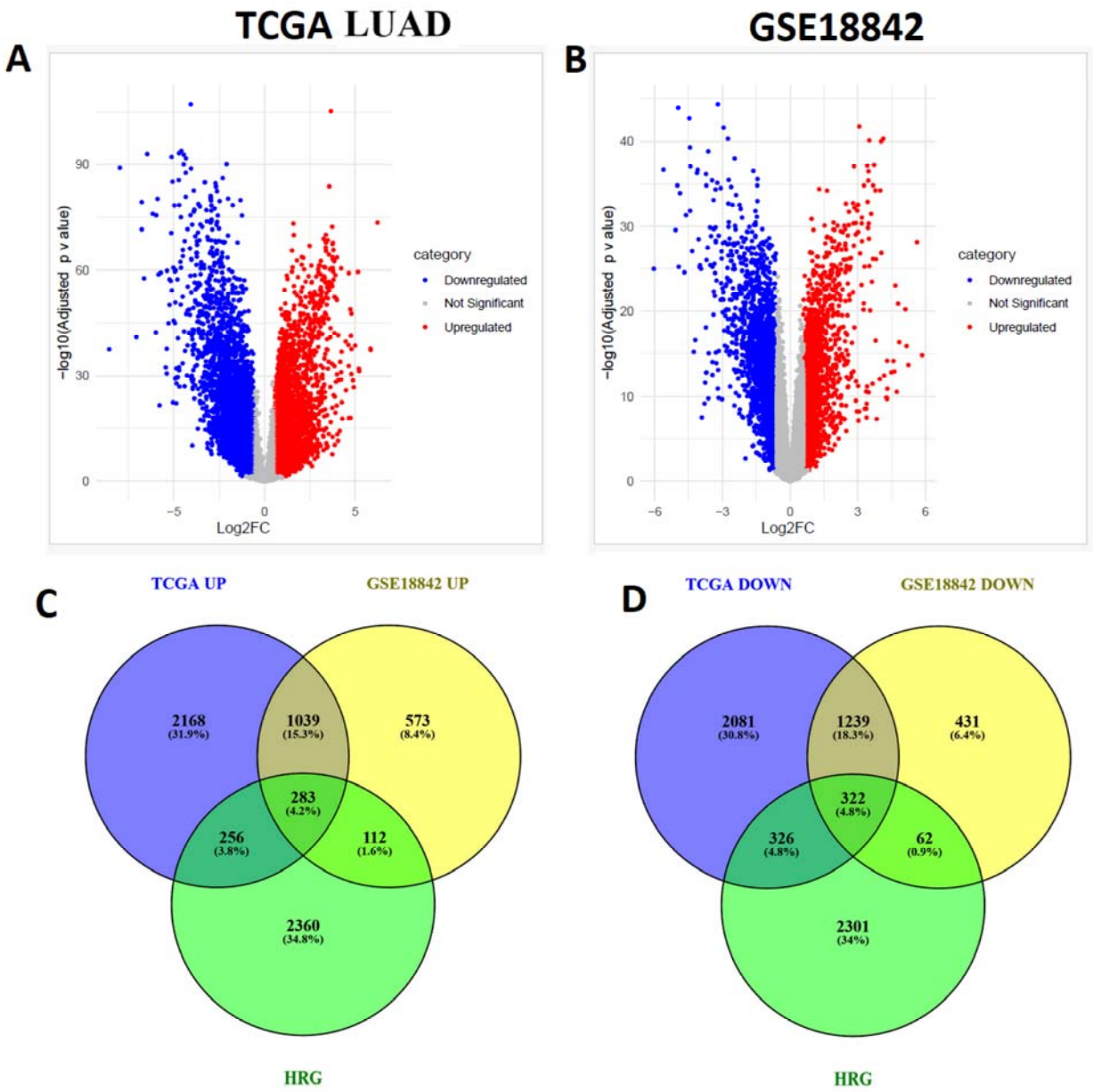

Figure 2. Volcano plots and Venn diagrams depicting DEGs and HRDEGs in LUAD.A. Volcano plot of DEGs in the TCGA LUAD cohort. **B.** Volcano plot of DEGs in the GSE18842 dataset, illustrating differential gene expression in LUAD. **C.** Venn diagram showing the overlap of upregulated HRDEGs in LUAD. **D**. Venn diagram illustrating the overlap of downregulated HRDEGs in LUAD.TCGA UP: TCGA-LUAD upregulated; TCGA DOWN: TCGA-LUAD downregulated; HRG: hypoxia-related genes

Table 1. The top ten upregulated and downregulated HRDEGs in TCGA and GSE18842

Regulatory status	Gene ID	Gene Symbol	TCGA		GSE18842		Name of the genes
			logFC	Adjusted P Value	logFC	Adjusted P Value	
Upregulated	1591	*CYP24A1*	5.211	8.81E-33	1.293	9.12E-06	cytochrome P450 family 24 subfamily A member 1
	768	*CA9*	4.929	2.12E-27	1.749	3.30E-13	carbonic anhydrase 9
	4322	*MMP13*	4.885	2.07E-29	1.825	1.41E-07	matrix metallopeptidase 13
	6696	*SPP1*	4.739	1.41E-49	2.540	2.92E-20	secreted phosphoprotein 1
	1300	*COL10A1*	4.653	6.9E-60	3.547	8.02E-21	collagen type X alpha 1 chain
	4312	*MMP1*	4.651	1.47E-33	5.110	5.85E-21	matrix metallopeptidase 1
	1917	*EEF1A2*	4.297	1.69E-18	0.989	2.14E-05	eukaryotic translation elongation factor 1 alpha 2
	26585	*GREM1*	4.257	1.7E-37	4.666	8.94E-24	"gremlin 1, DAN family BMP antagonist"
	5307	*PITX1*	4.233	9.46E-32	1.629	6.43E-17	paired like homeodomain 1
	4321	*MMP12*	4.085	1.72E-29	5.626	7.05E-29	matrix metallopeptidase 12
Downregulated	6440	*SFTPC*	-8.560	3.4E-38	-6.0378	1.01E-25	surfactant protein C
	6532	*SLC6A4*	-7.971	7.8E-90	-1.9304	1.49E-15	solute carrier family 6 member 4
	177	*AGER*	-6.765	2.62E-72	-4.9568	1.01E-44	advanced glycosylation end-product specific receptor
	2167	*FABP4*	-6.160	9.71E-77	-3.4366	5.77E-26	fatty acid binding protein 4
	7356	*SCGB1A1*	-5.786	2.46E-22	-3.9076	3.06E-08	secretoglobin family 1A member 1
	2277	*VEGFD*	-5.008	2.11E-46	-4.4324	4.79E-40	vascular endothelial growth factor D
	3043	*HBB*	-4.916	1.54E-51	-2.5255	1.07E-25	hemoglobin subunit beta
	729238	*SFTPA2*	-4.863	6.09E-23	-3.7907	6.99E-10	surfactant protein A2
	361	*AQP4*	-4.688	1.29E-27	-3.9426	9.98E-26	aquaporin 4
	7123	*CLEC3B*	-4.241	2.27E-72	-4.4159	8.41E-38	C-type lectin domain family 3 member B

HRDEGs are associated with cellular processes such as cell cycle and metabolism.

Figure 3 illustrates the pathways significantly enriched by the upregulated genes, with a false discovery rate (FDR) < 0.05. These pathways highlight key biological processes and molecular mechanisms potentially associated with tumorigenesis (**Supplementary Table S5**). Notably, the

cell cycle (hsa04110), biosynthesis of amino acids (hsa01230), and carbon metabolism (hsa01200) are central to cellular growth and energy production. The p53 signaling pathway (hsa04115) and cellular senescence (hsa04218) are also implicated, reflecting the regulation of cell death and aging processes. Other enriched pathways, such as glycolysis/gluconeogenesis (hsa00010) and HIF-1 signaling (hsa04066), suggest alterations in metabolic pathways and hypoxic responses often observed in cancer. Additionally, pathways related to cancer progression, such as central carbon metabolism in cancer (hsa05230), pathways in cancer (hsa05200), and microRNAs in cancer (hsa05206), are also prominently featured, highlighting the complex molecular interactions in cancer biology. Other enriched pathways include DNA replication (hsa03030), mismatch repair (hsa03430), and glutathione metabolism (hsa00480), which are critical for genome stability and oxidative stress responses. The statistical analysis of upregulated pathways is tabulated in Supplementary Table S5. These results emphasize the multifaceted nature of the upregulated genes and their involvement in various cellular functions relevant to cancer development.

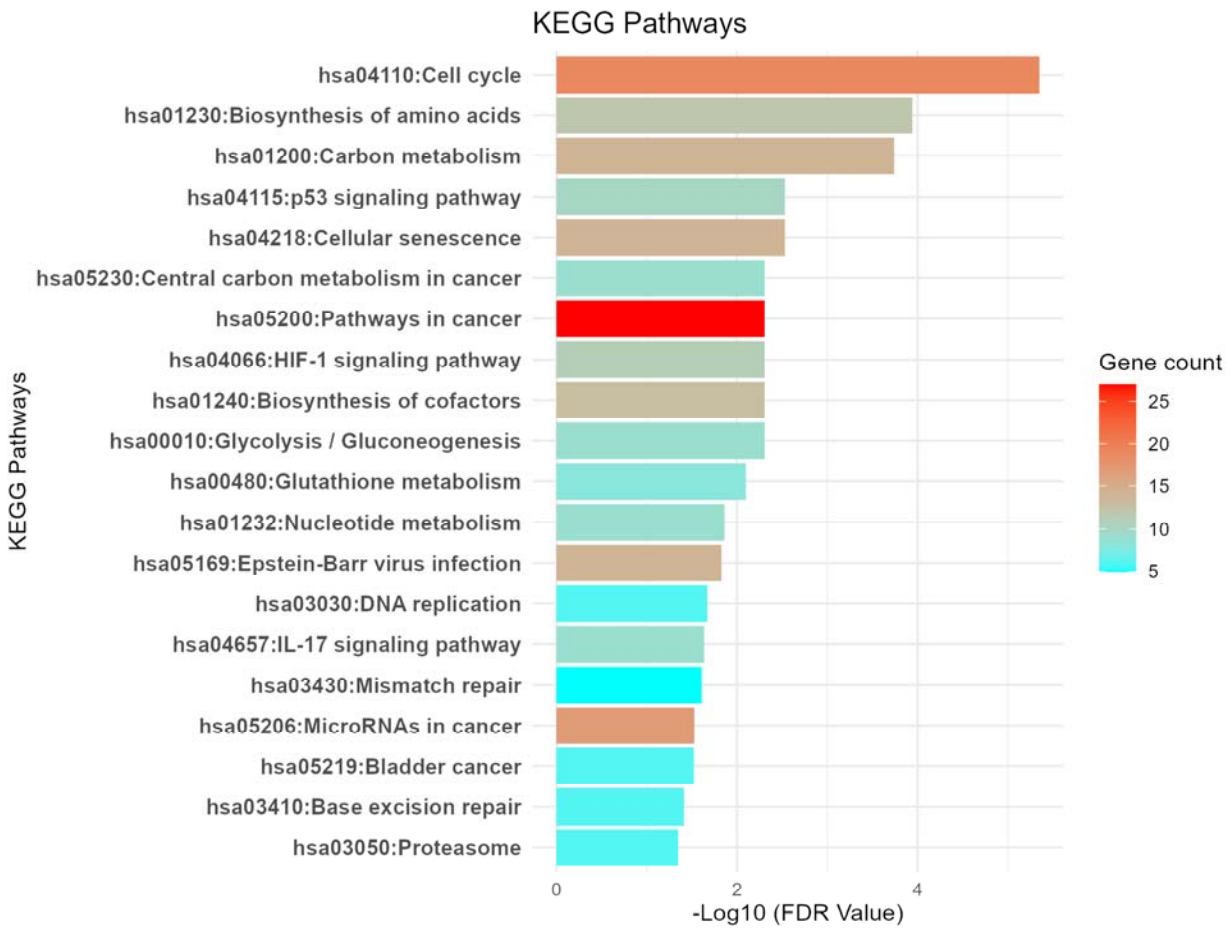

Figure 3. Significantly enriched pathways associated with the upregulated genes (FDR < 0.05). DEG upregulated were analyzed for functional pathways using DAVID.

The top enriched pathway, the Cell Cycle (**Figure 4**), with a highly significant p-value of 4.51E-06. This pathway is critical for regulating cell division and proliferation. The genes enriched within this pathway, including *PCNA*, *MCM7*, *CDKN2A*, *PRKDC*, *HDAC1*, *CDC6*, and others such as *CDK4*, *CHEK1*, and *E2F3*, play pivotal roles in cell cycle aberration. These genes are integral to maintaining proper cell cycle regulation, and their upregulation suggests a potential disruption in normal cell division processes, which is commonly associated with tumorigenesis. The enrichment of these genes further underscores the importance of the cell cycle in hypoxic lung cancer biology.

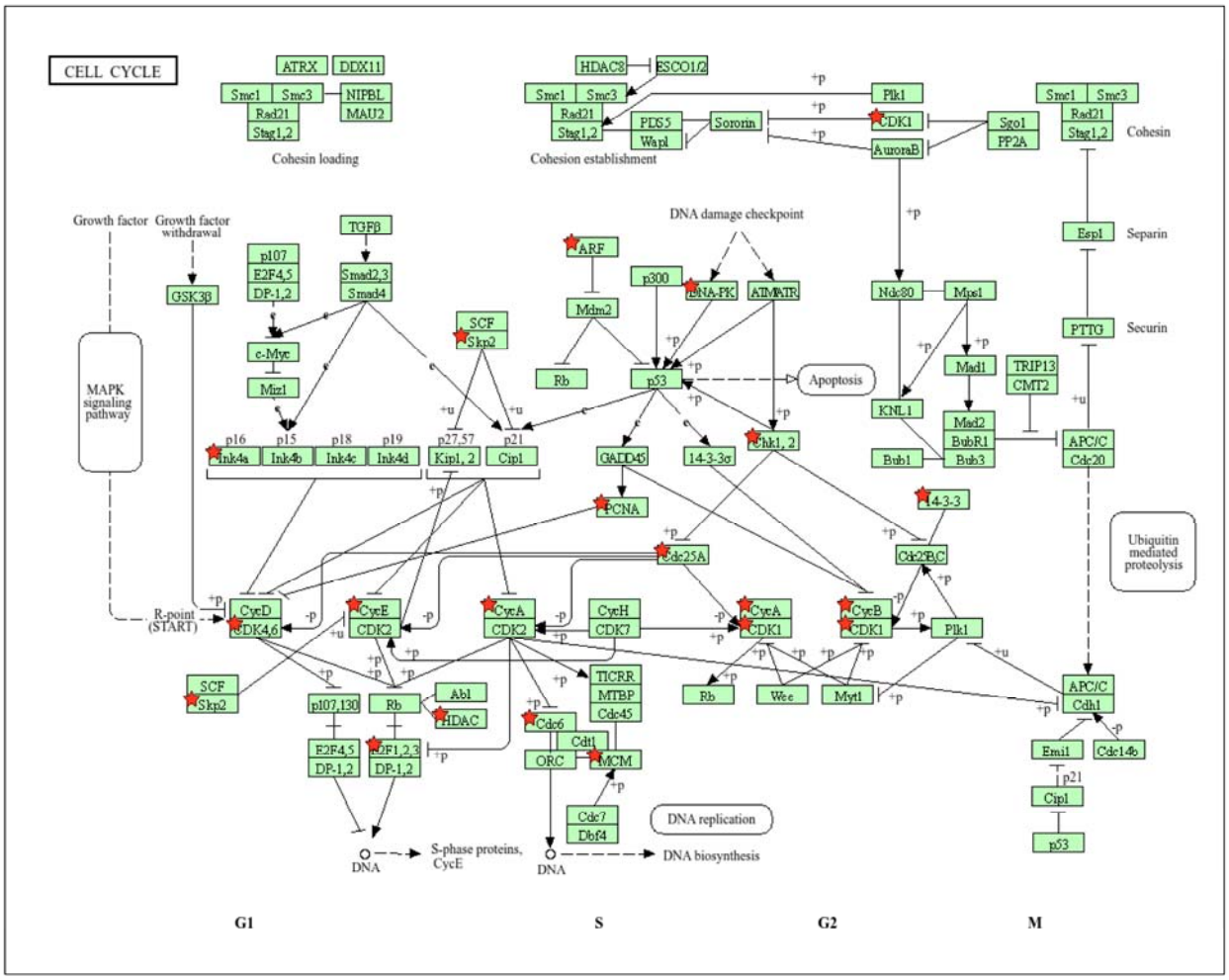

Figure 4: KEGG pathway illustrating the Cell Cycle pathway from DAVID, with upregulated genes marked by red stars.

Similar to the Cell Cycle pathway, another significantly enriched pathway is the HIF-1 signaling pathway (hsa04066), with genes such as *LDHA*, *EGLN3*, *SLC2A1*, *EIF4EBP1*, *PGK1*, *TIMP1*, *ENO1*, *ALDOA*, *GAPDH*, *PFKP*, and *PDK1* being upregulated (**Figure 5**). The upregulation of these genes suggests a critical role of hypoxia in lung cancer, as these genes are involved in metabolic adaptation to low oxygen conditions (25). This highlights the importance of hypoxia-

induced signaling in promoting tumor survival and progression through altered cellular metabolism.

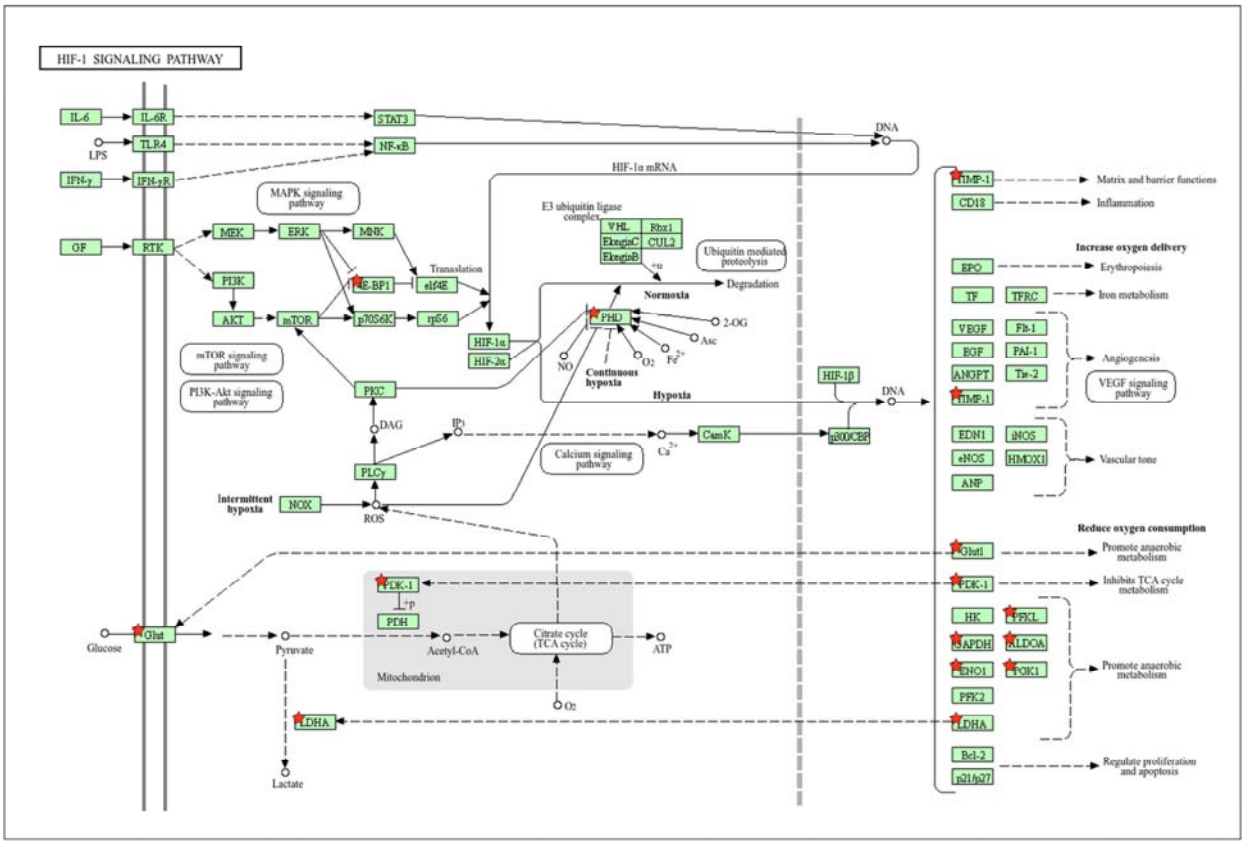

Figure 5: KEGG pathway illustrating the HIF-1 signaling pathway from DAVID, with upregulated genes marked by red stars. Upregulated genes, such as *LDHA, EGLN3, SLC2A1, EIF4EBP1, PGK1, TIMP1, ENO1, ALDOA, GAPDH, PFKP, and PDK1*, are shown with red stars, indicating their involvement in metabolic reprogramming and cellular adaptation to low oxygen conditions.

In addition to the upregulated genes, we observed that the downregulated genes are predominantly associated with immune-related pathways and signaling processes. As illustrated in **Figure 6**, several immune-related pathways are significantly affected, indicating a potential

suppression of immune responses in lung cancer. Key pathways include the TNF signaling pathway (hsa04668), Cytokine-cytokine receptor interaction (hsa04060), and IL-17 signaling pathway (hsa04657), all of which play essential roles in immune activation and inflammation. Other important pathways such as Toll-like receptor signaling (hsa04620), JAK-STAT signaling (hsa04630), and Natural killer cell-mediated cytotoxicity (hsa04650) are also downregulated, suggesting that the immune system's ability to recognize and eliminate cancer cells may be impaired. The statistical analysis of upregulated pathways is tabulated in **Supplementary Table S6**. These findings suggests a potential immune evasion mechanism in lung cancer, where the downregulation of key immune pathways may allow tumors to escape immune surveillance and progress unchecked.

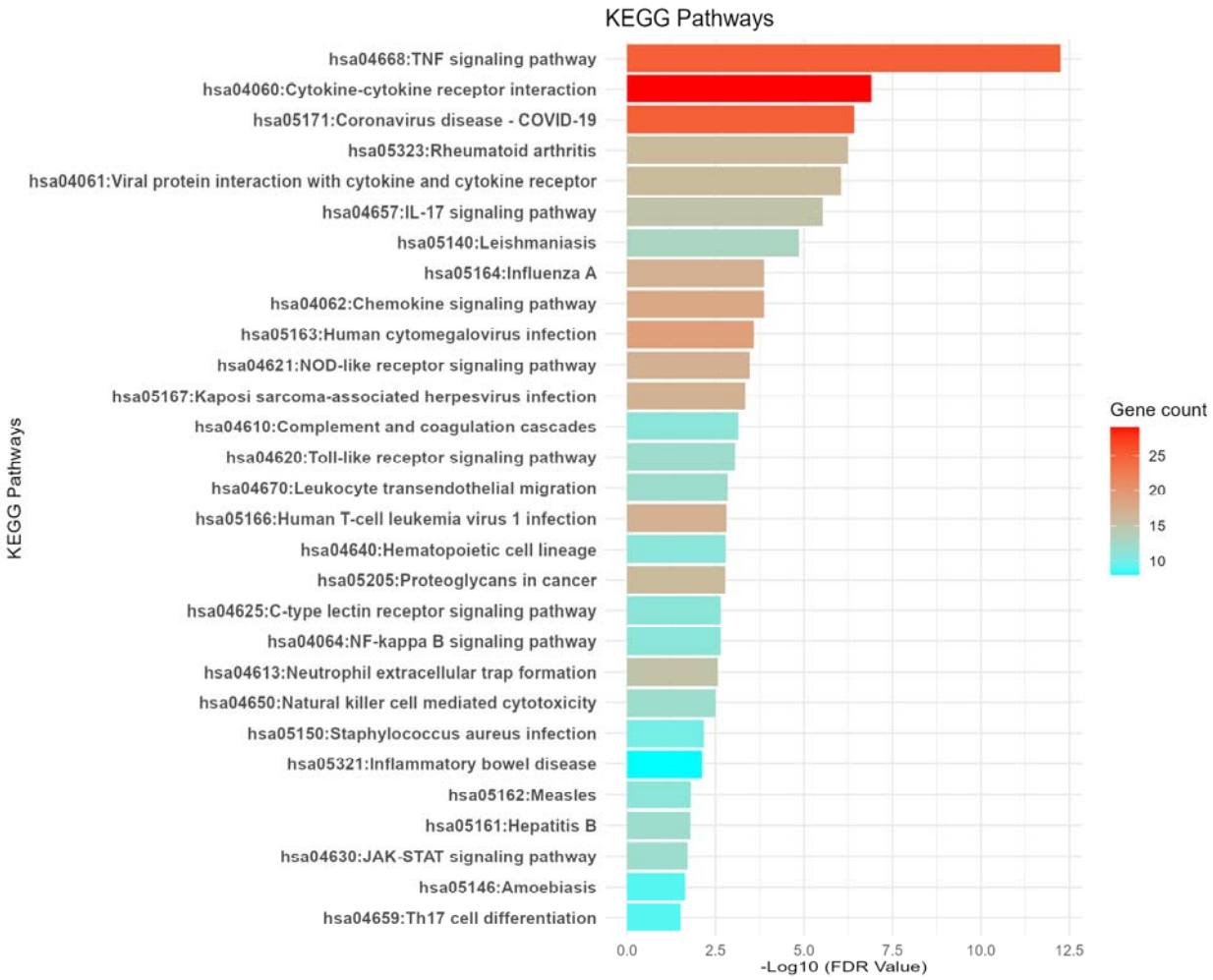

Figure 6: Immune-associated pathways enriched in the downregulated genes. This figure illustrates the major immune-related pathways that are significantly downregulated in lung cancer.

Explorations of hub HRDEGs

Next, we conducted a Protein-Protein Interaction (PPI) analysis by inputting all the hypoxia-related differentially expressed genes (DEGs) into the STRING database. The primary PPI network consisted of 600 nodes and 9,281 edges, with an average node degree of 30.9 (**Figure 7**). The PPI enrichment p-value was found to be < 1.0e-16, indicating a highly significant

interaction among the hypoxia-related genes. Based on a degree of interaction greater than 10, we identified the hub genes within the network. After identifying the hub genes based on the degree of interaction, we found that the top hub genes include *GAPDH, IL6, TNF, IL1B, MMP9, JUN, CCL2, TLR4, FOS, PTGS2, PECAM1, CDH1, HSP90AB1, PTPRC, ICAM1, FGF2, PPARG, ITGAM, CXCL12, and KDR*. The list of all interacted genes and their degree of interaction provided in the **Supplementary Table S7**. These genes play pivotal roles in key biological processes such as inflammation, immune response, cell signaling, and tumor progression. **Figure 8A** illustrates the interaction network of the top 50 hub genes an, highlighting their interconnections and potential involvement in the molecular pathways that drive lung cancer progression. We further identified 201 common upregulated hub genes and 224 common downregulated hub genes, which were shared across the datasets. These genes represent key molecular players in the tumorigenic processes of lung cancer, with their dysregulation potentially contributing to cancer progression. The results of this analysis are presented in **Figure 8B** and are detailed in **Supplementary Table S7**.

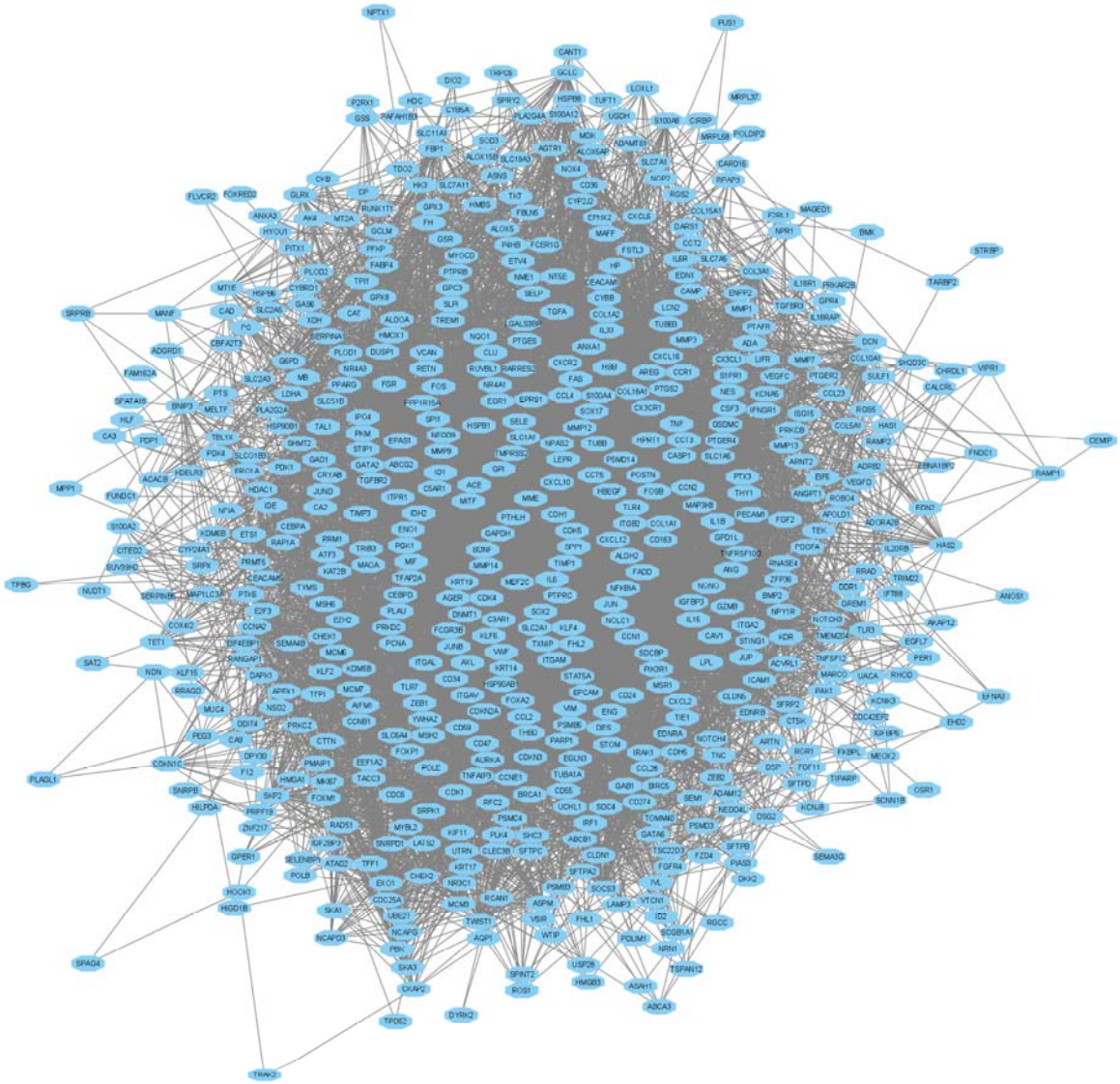

Figure 7. Primary Protein-Protein Interaction (PPI) network of hypoxia-related differentially expressed genes (DEGs) generated using STRING. The network consists of 600 nodes and 9,281 edges, with an average node degree of 30.9.

The top upregulated hub genes identified in this analysis include *MMP9*, *CDH1*, *HSP90AB1*, *SOX2*, *CDKN2A*, *SPP1*, *EZH2*, *TIMP1*, *CXCL10*, *COL1A1*, *HDAC1*, *BRCA1*, and *CDK4*. These genes are involved in critical processes such as tumor invasion, immune modulation, cell cycle regulation, and epigenetic changes. The top downregulated hub genes identified in this analysis *include IL6*, *TNF*, *IL1B*, *JUN*, *CCL2*, *TLR4*, *FOS*, *PTGS2*, *PECAM1*, *PTPRC*, *ICAM1*, *FGF2*,

PPARG, *ITGAM*, *CXCL12*, and *KDR*. These genes are primarily involved in immune response, inflammation, and cellular signaling pathways.

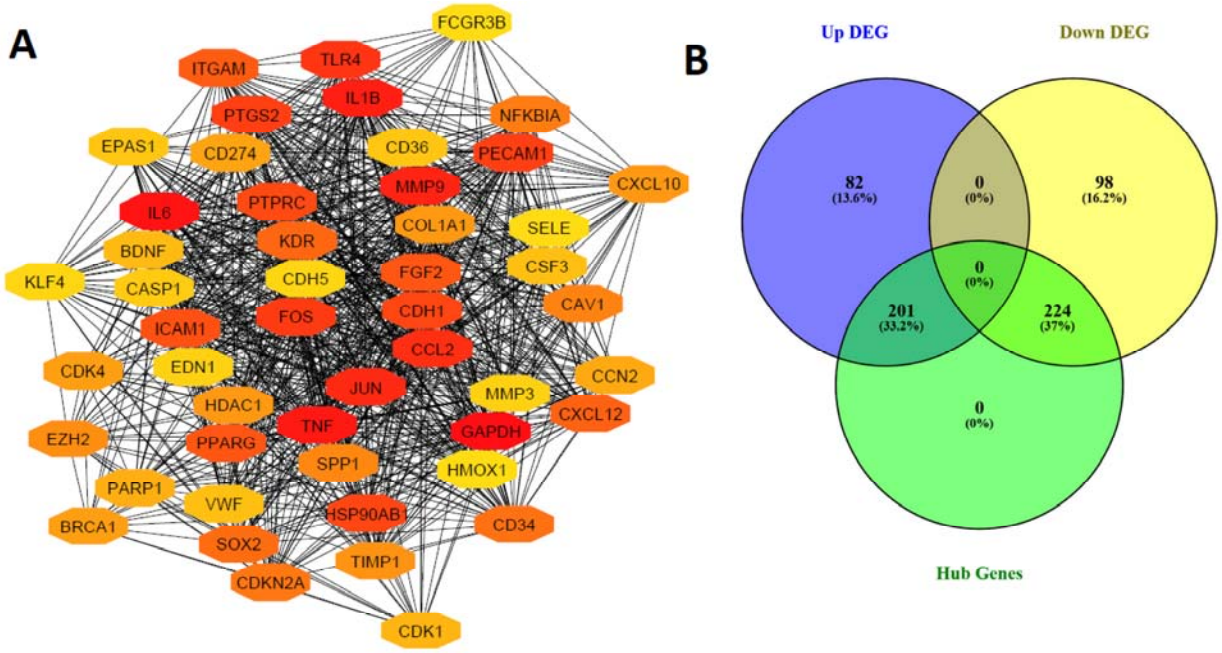

Figure 8. Protein-Protein Interaction (PPI) Network of Hub Genes. A. Interaction network of the top 50 hub genes identified from the PPI analysis. B. Common hub genes shared between the upregulated and downregulated gene sets.

Exploration of independent prognostic HRDEGs

We first conducted Kaplan-Meier survival analysis on all hub genes and identified 174 significant genes that were associated with survival (**Supplementary Table S8**). The following seven genes (Identified by Univariate regression and LASO)—*ADAM12* (HR=1.39, P=0.02), *CCNE1* (HR=1.43, P=0.01), *DSG2* (HR=1.58, P=0.002), *EIF6*(HR=1.49, P=0.008), EXO1

(HR=1.54, P=0.003), *IGF2BP3* (HR=1.6, P=0.001), and *RAD51* (HR=1.37, P=0.03)—are identified as upregulated hub genes in lung cancer (**Figure 9A**).

The upregulated group, categorized based on median expression levels, is associated with worse survival outcomes. Increased expression of these genes is correlated with poorer prognosis, suggesting that they may play a critical role in tumor progression and could serve as potential biomarkers for identifying high-risk patients with lung cancer. The following ten genes ((Identified by Univariate regression and LASO))—*ABCB1*(HR=0.71, P=0.02), *ADRB2*(HR=0.67, P=0.008), *ALDH2*(HR=0.66, P=0.006), *CAT*(HR=0.73, P=0.03), *CLEC3B*(HR=0.67, P=0.006), *FBLN5*(HR=0.64, P=0.003), *MAP3K8*(HR=0.67, P=0.006), *PIK3R1*(HR=0.64, P=0.003), *SFTPD*(HR=0.68, P=0.01), and *SOD3*(HR=0.75, P=0.04)—are identified as downregulated hub genes in lung cancer.

A

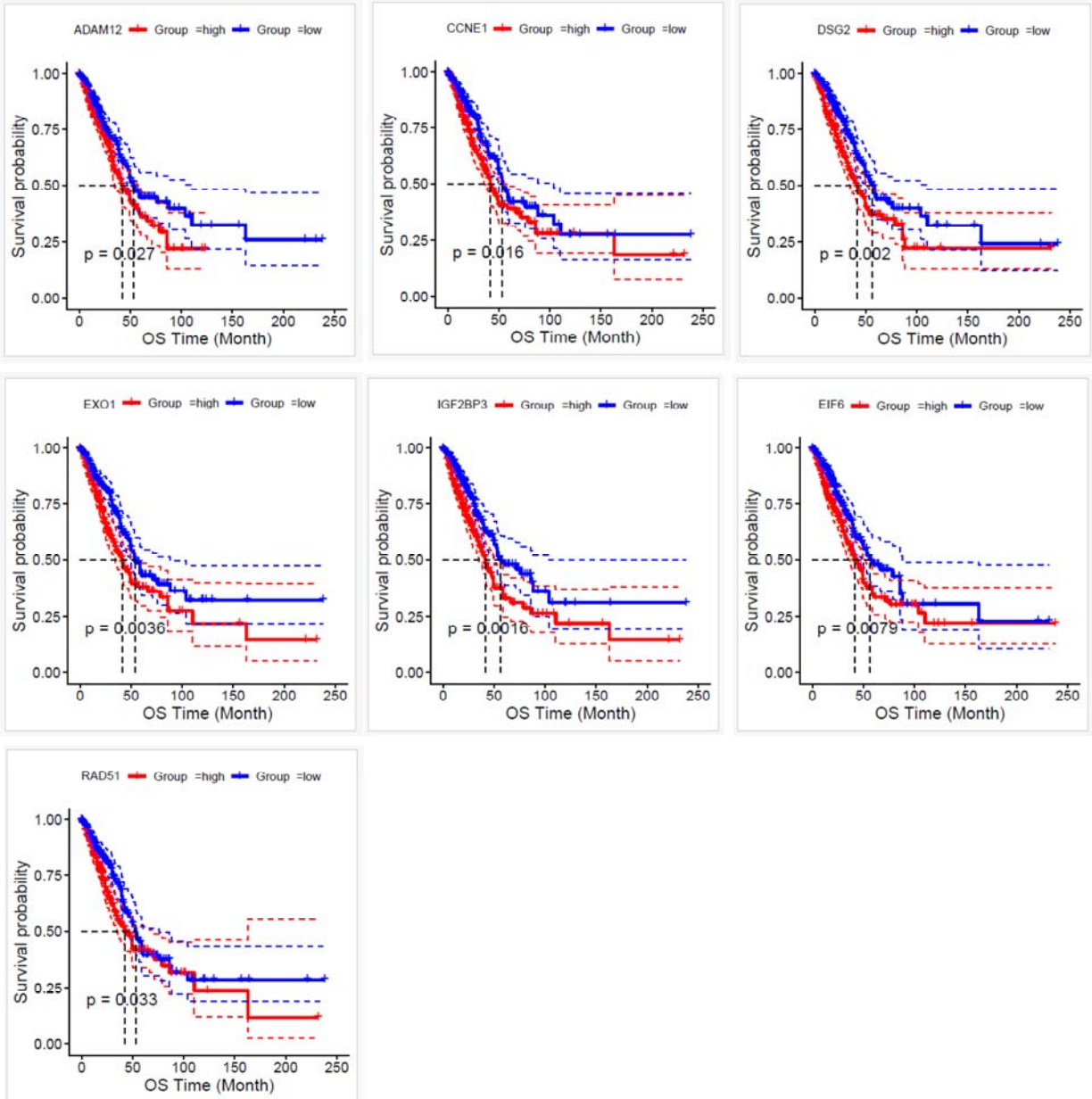
ADAM12 Group =high Group =low
p = 0.027
CCNE1 Group =high Group =low
p = 0.016
DSG2 Group =high Group =low
p = 0.002
EXO1 Group =high Group =low
p = 0.0036
IGF2BP3 Group =high Group =low
p = 0.0016
EIF6 Group =high Group =low
p = 0.0079
RAD51 Group =high Group =low
p = 0.033
Survival probability
OS Time (Month)

378

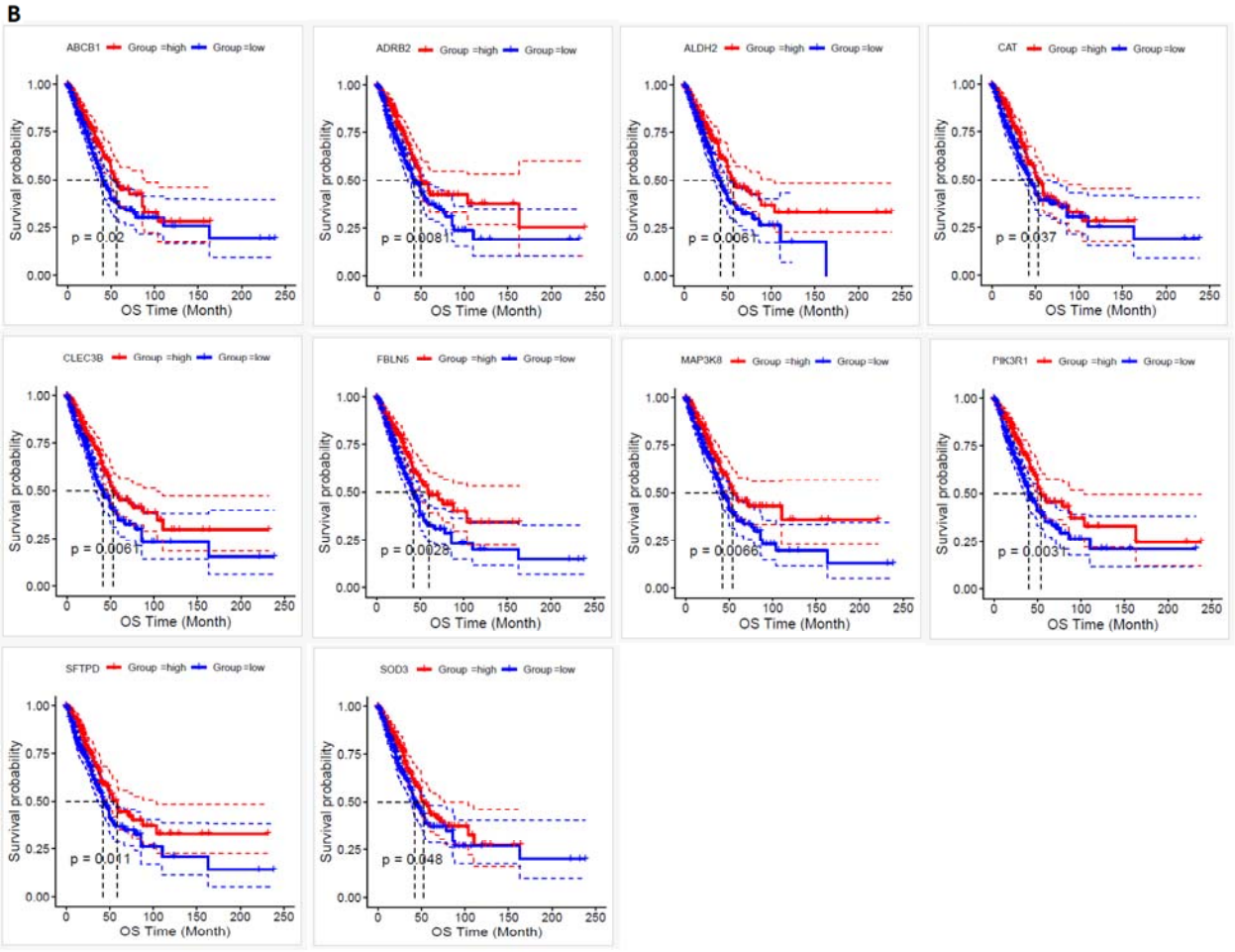

Figure 9. Kaplan-Meier Survival Analysis of Upregulated and Downregulated Hub Genes in Lung Cancer. A. Kaplan-Meier survival analysis of the group of upregulated hub genes, showing their significant association with survival in lung cancer patients. (B) Kaplan-Meier survival analysis of the group of downregulated hub genes, demonstrating their significant impact on survival outcomes.

To refine this list, we performed univariate regression analysis, which revealed 106 genes with statistically significant associations (**Supplementary Table S9)**. Subsequently, we applied Lasso regression to the consistently upregulated and downregulated genes to identify key genes with

non-zero coefficients. This analysis led to the identification of 17 key genes: *ADRB2*, *ALDH2*, *CAT*, *CCNE1*, *MAP3K8*, *DSG2*, *EIF6*, *ABCB1*, *PIK3R1*, *RAD51*, *SFTPD*, *SOD3*, *CLEC3B*, *ADAM12*, *EXO1*, *FBLN5*, and *IGF2BP3*. The univariate regression analysis and LASSO regression analysis depicted in the **Figure 10** and **Figure 11**, respectively.

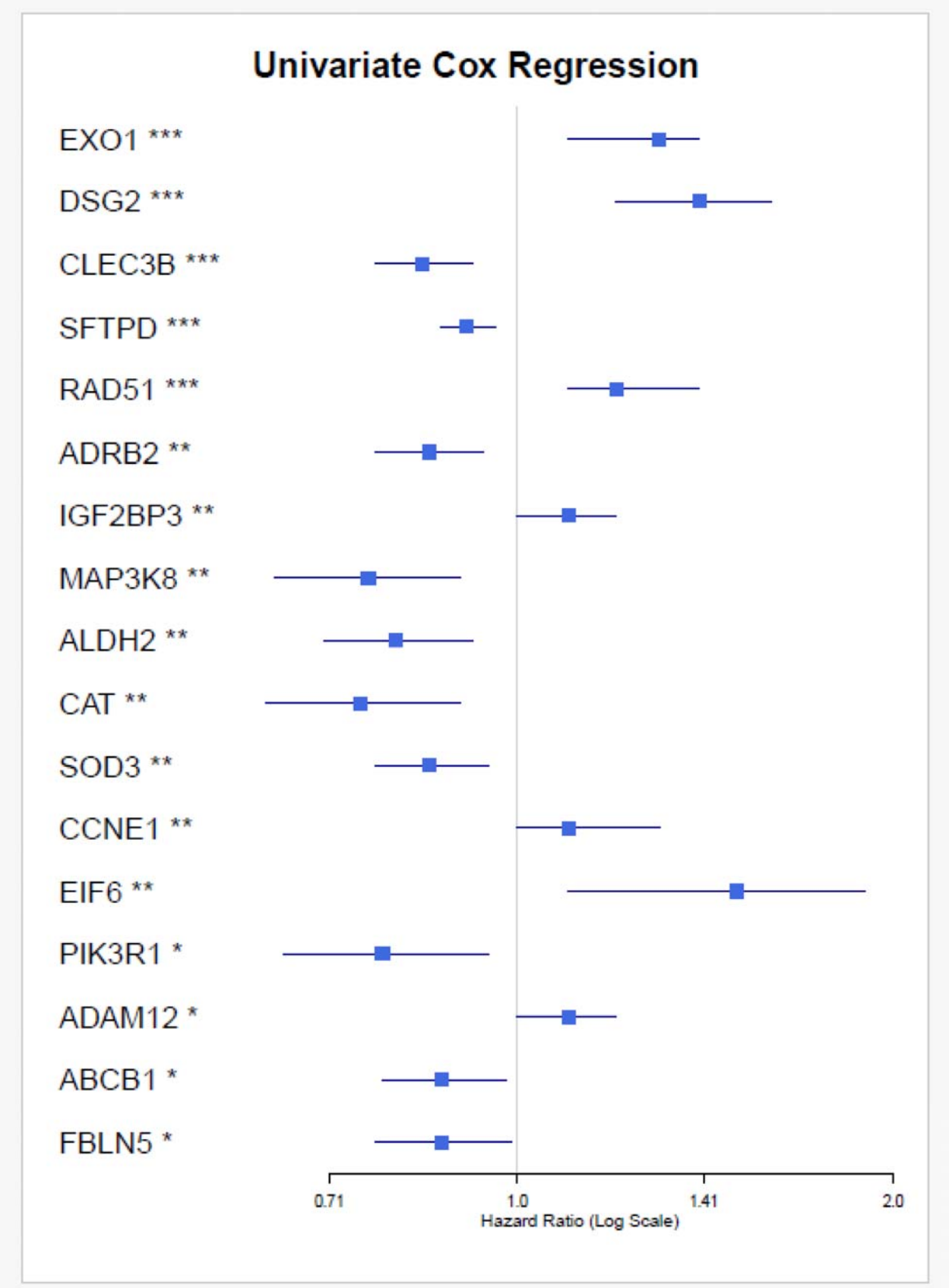
Univariate Cox Regression
EXO1 ***
DSG2 ***
CLEC3B ***
SFTPD ***
RAD51 ***
ADRB2 **
IGF2BP3 **
MAP3K8 **
ALDH2 **
CAT **
SOD3 **
CCNE1 **
EIF6 **
PIK3R1 *
ADAM12 *
ABCB1 *
FBLN5 *
0.71
1.0
1.41
2.0
Hazard Ratio (Log Scale)

394

Figure 10: The results of univariate Cox regression analysis for hub genes in lung cancer patients. Each gene's hazard ratio (HR) with 95% confidence interval (CI) is displayed, indicating the association between gene expression and patient survival.

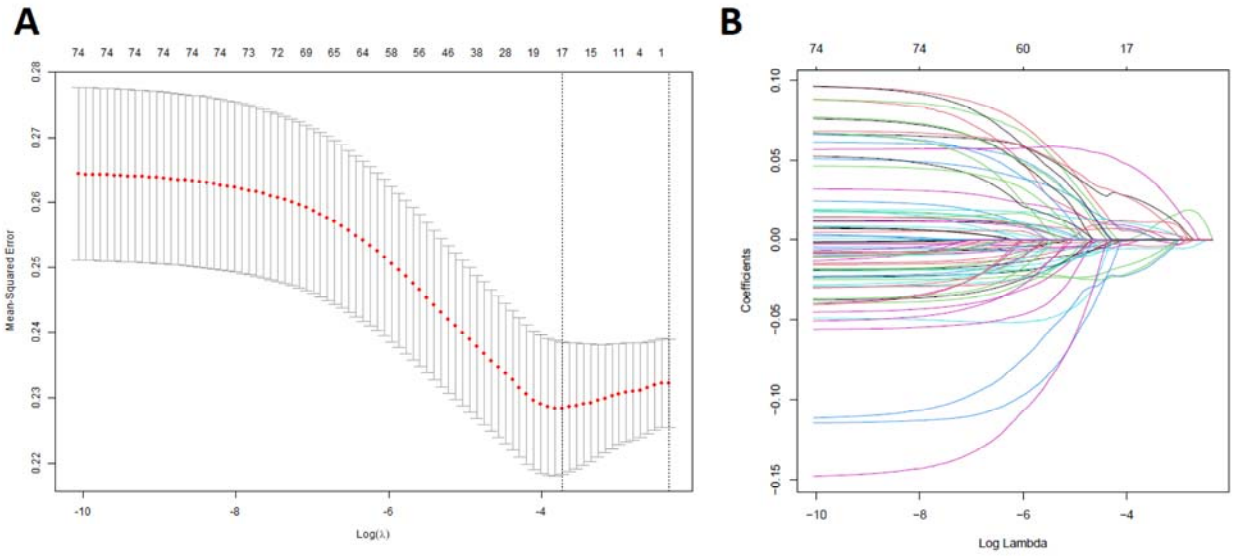

Figure 11: Lasso Regression Analysis of Key Genes. Identification of key genes through Lasso regression. (A) Lasso coefficients for each gene selected through Lasso regression. The plot shows the evolution of the coefficients for each gene as the regularization penalty (lambda) increases. (B) Log(lambda) vs. coefficients plot demonstrating the relationship between the log-transformed lambda values and the corresponding coefficients.

Furthermore, a multivariate Cox regression analysis was conducted to identify independent prognostic factors. The results indicated that *DSG2*, *EIF6*, and *EXO1* emerged as independent prognostic factors (**Figure 12**). The multivariate model demonstrated a significant fit, with the following statistics: Concordance = 0.657 (SE = 0.024), Likelihood ratio test = 50.39 on 17

degrees of freedom (df), p = 4e-05, Wald test = 48.47 on 17 df (p = 7e-05), and Score (logrank) test = 48.73 on 17 df (p = 7e-05). *DSG2* (HR = 1.238, p = 0.012), *EIF6* (HR = 1.387, p = 0.046), and *EXO1* (HR = 1.257, p = 0.047) all have hazard ratios greater than 1, indicating that higher expression of these genes is associated with poorer survival outcomes.

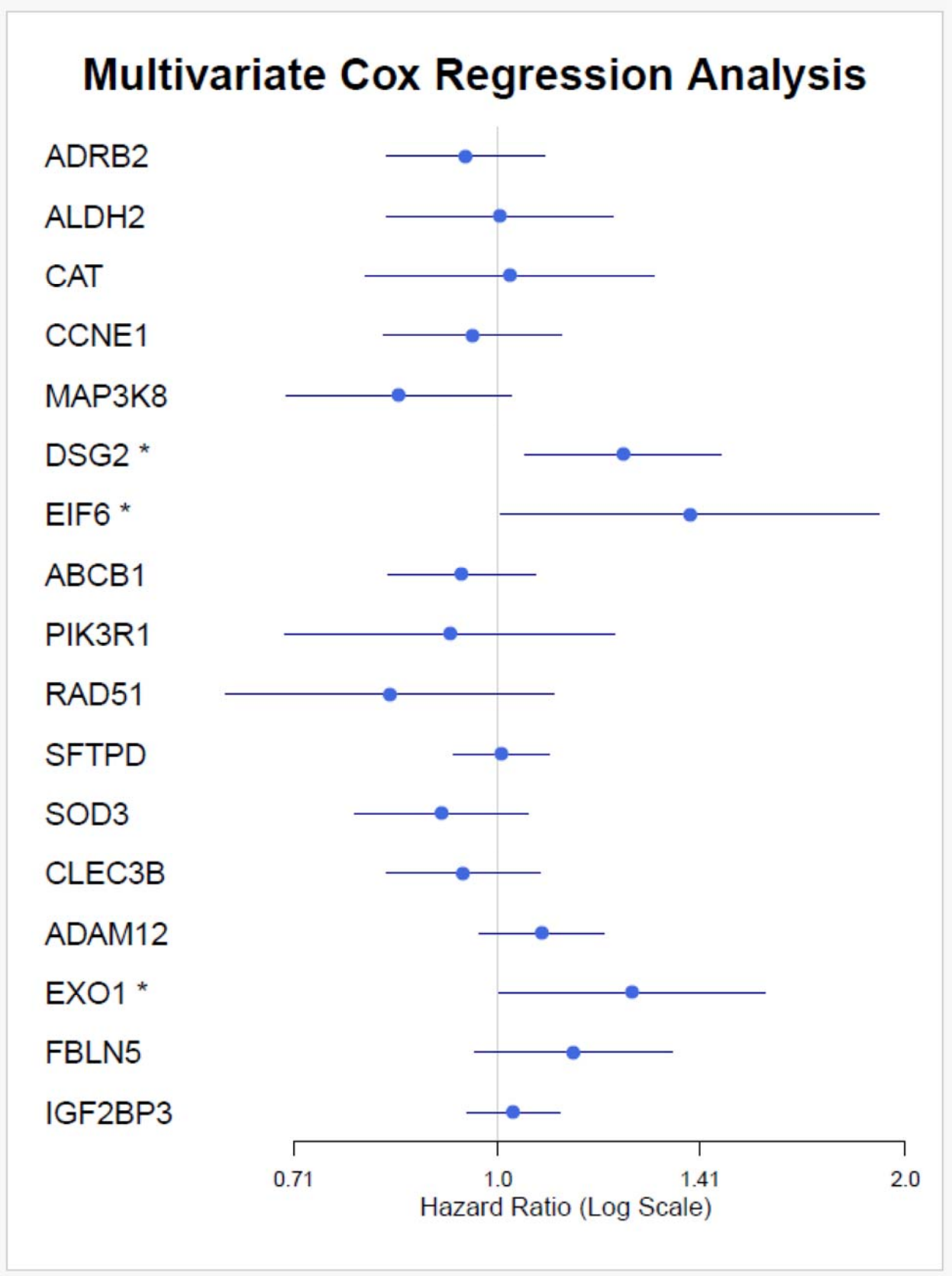
Multivariate Cox Regression Analysis
ADRB2
ALDH2
CAT
CCNE1
MAP3K8
DSG2 *
EIF6 *
ABCB1
PIK3R1
RAD51
SFTPD
SOD3
CLEC3B
ADAM12
EXO1 *
FBLN5
IGF2BP3
0.71
1.0
1.41
2.0
Hazard Ratio (Log Scale)

415

Figure 12: Multivariate Cox regression analysis identifying independent prognostic factors.

Validation of prognostic value in an independent cohort

To validate the prognostic relevance of *DSG2*, *EIF6*, and *EXO1* in our risk model, we utilized the independent dataset GSE13213 through the SurvExpress platform (24). The analysis revealed that all three genes maintained a significant association with patient prognosis in this external cohort. Specifically, DSG2 (coefficient: 0.2795, p-value: 0.05), EIF6 (coefficient: 0.8356, p-value: 0.019), and EXO1 (coefficient: 0.7033, p-value: 0.001) were all positively correlated with poor survival outcomes. The overall model performance was statistically robust, as indicated by a Log-Rank p-value < 0.001 and a hazard ratio (HR) of 3.19, underscoring the model's strong prognostic power in stratifying patients.

Further stratification of the cohort into high-risk and low-risk groups based on the risk scores revealed a significant survival difference, with patients in the high-risk group exhibiting markedly shorter survival times compared to those in the low-risk group (**Figure 13A**). Moreover, expression analysis confirmed that DSG2, EIF6, and EXO1 were significantly upregulated in the high-risk group, consistent with our primary findings (**Figure 13B**). These validation results provide strong support for the clinical applicability of the proposed gene signature and reinforce the role of these three genes as potential biomarkers for risk stratification and prognosis in lung cancer.

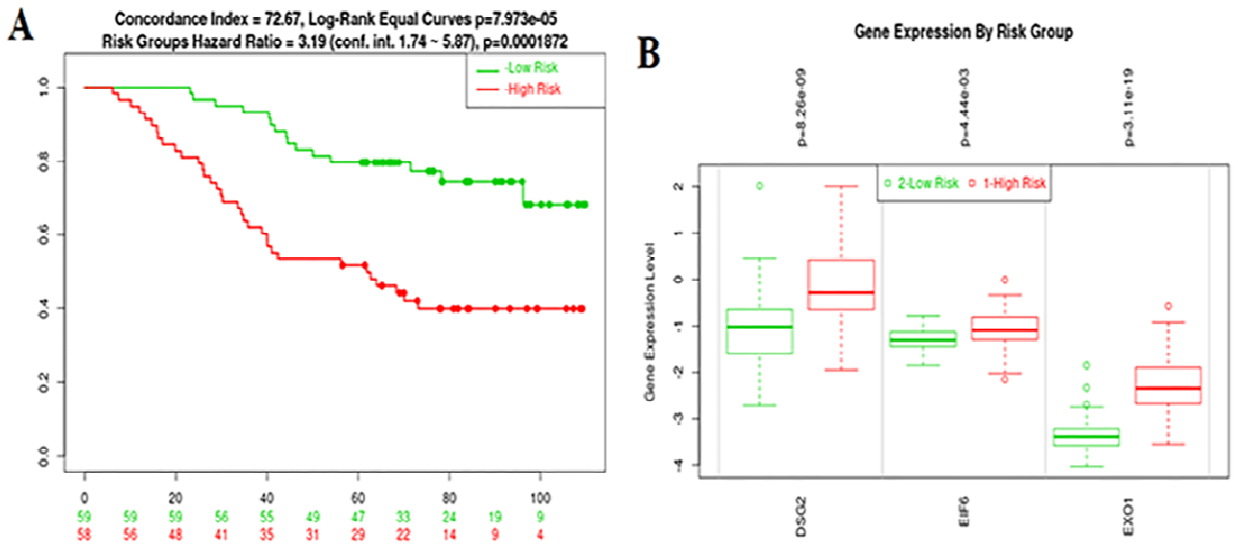

Figure 13. Validation of Prognostic Gene Signature Using Independent Cohort (GSE13213). A: Survival Analysis Based on Risk Groups in GSE13213 Dataset utilizing SurvExpress platform. B: Expression Levels of DSG2, EIF6, and EXO1 in High- and Low-Risk Groups.

Discussion

Lung adenocarcinoma remains one of the leading causes of cancer-related mortality worldwide, with hypoxia recognized as a key contributor to tumor progression, metastasis, and therapy resistance. In this study, we comprehensively analyzed hypoxia-related differentially expressed genes (HRDEGs) in LUAD and identified 283 upregulated and 322 downregulated HRDEGs, reflecting the broad impact of hypoxic signaling on multiple cellular processes. Functional enrichment and protein-protein interaction analyses revealed that upregulated genes were primarily involved in cancer-related and cellular signaling pathways, whereas downregulated

genes were enriched in immunity-associated pathways, highlighting the dual role of hypoxia in promoting tumor growth while modulating immune responses.

The enrichment of cell cycle–related genes, including *PCNA*, *MCM7*, *CDKN2A*, *PRKDC*, *HDAC1*, *CDC6*, *CDK4*, *CHEK1*, and *E2F3*, highlights a pronounced dysregulation of cell cycle control mechanisms in lung cancer. These genes are central to DNA replication, cell cycle progression, and checkpoint regulation, ensuring genomic integrity under normal physiological conditions (26-28). Their coordinated upregulation suggests enhanced proliferative capacity and impaired checkpoint surveillance, which are hallmark features of tumorigenesis. In particular, aberrant activation of CDKs and E2F transcription factors can drive uncontrolled entry into the S phase (29), while altered expression of DNA damage response genes such as *CHEK1* and *PRKDC* may allow cancer cells to bypass critical repair checkpoints, thereby promoting genomic instability (30, 31). Collectively, these findings underscore the pivotal role of cell cycle dysregulation in lung cancer development and progression.

In addition to cell cycle alterations, the HIF-1 signaling pathway (hsa04066) emerged as another significantly enriched pathway, with notable upregulation of genes including *LDHA*, *EGLN3*, *SLC2A1*, *EIF4EBP1*, *PGK1*, *TIMP1*, *ENO1*, *ALDOA*, *GAPDH*, *PFKP*, and *PDK1*. These genes are key mediators of cellular adaptation to hypoxic conditions and are closely associated with metabolic reprogramming in cancer. The elevated expression of glycolytic enzymes and glucose transporters, such as *SLC2A1* and *LDHA*, reflects a shift toward aerobic glycolysis (the Warburg effect), enabling tumor cells to sustain rapid growth in oxygen-deprived microenvironments (32). Taken together, the concurrent activation of cell cycle and HIF-1 signaling pathways suggests a coordinated mechanism by which lung cancer cells promote unchecked proliferation while adapting to hypoxic stress. These pathways may act synergistically to facilitate tumor

progression and aggressiveness, highlighting their potential as therapeutic targets and prognostic biomarkers in lung cancer.

Beyond the activation of oncogenic and metabolic programs, lung cancer was characterized by a marked suppression of immune-associated pathways, reflecting the establishment of an immunosuppressive tumor microenvironment (33). The coordinated downregulation of signaling cascades involved in cytokine communication, inflammatory responses, and immune cell activation indicates a weakened immune network within tumors (34). Furthermore, attenuation of pathways governing innate immune sensing and effector mechanisms suggests reduced recognition and clearance of malignant cells by immune surveillance systems (35). Such widespread impairment of immune signaling is consistent with tumor-driven immune evasion, in which cancer cells actively modulate immune pathways to avoid immune-mediated destruction (36). This immune suppression may not only facilitate tumor progression but also contribute to resistance to immune-based therapies, underscoring the critical role of immune pathway dysregulation in lung cancer pathogenesis (34). Interestingly, we have previously shown that HIF-1 suppresses NF-κB signalling (37), one of the pathways found to be significantly downregulated in the analysis of lung adenocarcinoma presented here.

Moreover, the top upregulated hub genes, including, *MMP9* and *SPP1* play key roles in extracellular matrix remodeling and metastasis (38, 39), while *CDH1* is important for maintaining cell-cell adhesion (40). Other upregulated hub genes, including *SOX2* and *EZH2* regulate stem cell-like properties and epigenetic modifications, contributing to cancer stem cell maintenance and progression (41, 42). *CDK4* and *CDKN2A* are crucial regulators of the cell cycle, promoting cell division and tumor growth (43, 44). *BRCA1* and *HDAC*1 are involved in DNA repair and chromatin remodeling (45, 46), while *CXCL10* and *TIMP1* are associated with

immune responses (47, 48). The upregulation of these hub genes highlights their critical roles in tumor progression and their potential as therapeutic targets in lung cancer. On the other hand, the downregulation of IL6, TNF, and IL1B suggests impaired inflammatory signaling (49), while *TLR4*, *FOS*, and *ICAM1* are involved in immune cell activation and adhesion (50, 51), indicating potential immune evasion mechanisms. *PECAM1* and *KDR* are associated with endothelial cell function and angiogenesis, both crucial for tumor vasculature (51, 52). The downregulation of *PPARG*, *ITGAM*, and *CXCL12* further highlights disruptions in immune regulation and cell migration (53-55). Overall, the downregulation of these hub genes suggests a weakened immune response, contributing to tumor progression and immune evasion in lung cancer.

Some of the survival associated genes are involved in the several cancers. For example, Li et al. reported that both the transcriptional and post-transcriptional expression levels of *ADAM12* are significantly elevated in tumor tissues compared to normal tissues. Furthermore, increased *ADAM12* expression was found to be associated with poor prognosis in patients with lung adenocarcinoma (56). Ma et al. found that *CCNE1* is upregulated in LUAD and that its knockdown suppresses tumor growth and metastasis. High *CCNE1* expression correlates with advanced stage, larger tumors, lymph node involvement, and poor prognosis (57). The downregulated group, categorized based on median expression levels, is associated with worse survival outcomes. Lower expression of these genes correlates with poorer prognosis, suggesting that their downregulation may contribute to tumor progression and aggressive cancer behavior (58, 59). These findings highlight the potential role of these downregulated genes in worsening survival outcomes and underscore their relevance as prognostic biomarkers for lung cancer. These genes, selected through Lasso, represent the most influential biomarkers for survival prediction, highlighting their potential roles in prognosis and therapeutic targeting.

By integrating survival analysis and regression modeling, we further identified *DSG2*, *EIF6*, and *EXO1* as independent prognostic factors, establishing a novel hypoxia-related gene signature that may inform both patient prognosis and therapeutic strategies in LUAD. Previous studies reported that independent prognostic factors are involved in the several cancer pathogeneses. Gong et al. reported that elevated *DSG2* expression is significantly associated with poor prognosis and reduced immune cell infiltration in various cancers (60). Zhu et al. found that overexpression of eIF6 regulates its downstream target, cell division control protein, contributing to oncogenesis. They also highlighted the potential of eIF6 as a diagnostic biomarker for cancer (61). Liu et al. identified *EXO1* as a significant biomarker with both prognostic and diagnostic value across multiple cancers, highlighting its potential as a therapeutic target and its role in immunomodulation within the tumor microenvironment (62, 63).These results further support the robustness of *DSG2*, *EIF6*, and *EXO1* as key genes in the prediction of survival, making them critical targets for future therapeutic strategies and prognostic modeling.

While numerous studies have reported associations between hypoxia-related genes and LUAD prognosis, our study identifies a novel three-gene signature comprising *DSG2*, *EIF6*, *and EXO1*, which has not been previously reported as a prognostic panel. This signature captures distinct aspects of hypoxia-driven tumor biology: DSG2 regulates cell adhesion and tumor progression (64), EIF6 controls translation initiation supporting rapid tumor growth under hypoxia (65), and EXO1 mediates DNA repair under replication stress, which is often exacerbated in hypoxic tumors (66). Importantly, these genes were validated in an independent cohort and may have clinical implications, as hypoxia influences the tumor microenvironment and response to immune checkpoint inhibitors. Thus, the *DSG2-EIF6-EXO1* signature not only provides robust

prognostic stratification but also offers mechanistic and potentially therapeutic insight, distinguishing it from previously reported hypoxia-related prognostic markers.

Conclusions

In conclusion, our analysis identifies *DSG2*, *EIF6*, and *EXO1* as key hypoxia-related genes with significant prognostic value in lung adenocarcinoma. These genes, through their involvement in hypoxia-related pathways, may play critical roles in tumor progression and patient survival. The findings suggest that *DSG2*, *EIF6*, and *EXO1* could serve as potential biomarkers for predicting patient outcomes and may offer novel therapeutic targets for improving prognosis in lung adenocarcinoma. Further validation of these genes in larger cohorts and clinical settings is necessary to confirm their utility in clinical practice.

Acknowledgements

We thank all the members of the scientific community for making their datasets public. This work was funded by a Wellcome Trust grant to SR (206293/Z/17/Z).

References

1. Zhang Y, Vaccarella S, Morgan E, Li M, Etxeberria J, Chokunonga E, et al. Global variations in lung cancer incidence by histological subtype in 2020: a population-based study. Lancet Oncol. 2023;24(11):1206-18.
2. Seguin L, Durandy M, Feral CC. Lung Adenocarcinoma Tumor Origin: A Guide for Personalized Medicine. Cancers (Basel). 2022;14(7).
3. Zhang C, Liu Y, Lu Y, Chen Z, Liu Y, Mao Q, et al. Identification of potential biomarkers for lung adenocarcinoma: a study based on bioinformatics analysis combined with validation experiments. Front Oncol. 2024;14:1425895.
4. Emami Nejad A, Najafgholian S, Rostami A, Sistani A, Shojaeifar S, Esparvarinha M, et al. The role of hypoxia in the tumor microenvironment and development of cancer stem cell: a novel approach to developing treatment. Cancer Cell Int. 2021;21(1):62.
5. Ciepla J, Smolarczyk R. Tumor hypoxia unveiled: insights into microenvironment, detection tools and emerging therapies. Clin Exp Med. 2024;24(1):235.
6. Petrova V, Annicchiarico-Petruzzelli M, Melino G, Amelio I. The hypoxic tumour microenvironment. Oncogenesis. 2018;7(1):10.

573 7. Child F, Frost J, Shakir D, Wilson JW, Rocha S. Transcription| regulation of gene transcription by
574 hypoxia-inducible factor 1α. 2021.
575 8. Bae T, Hallis SP, Kwak MK. Hypoxia, oxidative stress, and the interplay of HIFs and NRF2 signaling
576 in cancer. Exp Mol Med. 2024;56(3):501-14.
577 9. Bui BP, Nguyen PL, Lee K, Cho J. Hypoxia-Inducible Factor-1: A Novel Therapeutic Target for the
578 Management of Cancer, Drug Resistance, and Cancer-Related Pain. Cancers (Basel). 2022;14(24).
579 10. Gonzalez-Avila G, Sommer B, Flores-Soto E, Aquino-Galvez A. Hypoxic Effects on Matrix
580 Metalloproteinases' Expression in the Tumor Microenvironment and Therapeutic Perspectives. Int J Mol
581 Sci. 2023;24(23).
582 11. Roy S, Kumaravel S, Sharma A, Duran CL, Bayless KJ, Chakraborty S. Hypoxic tumor
583 microenvironment: Implications for cancer therapy. Exp Biol Med (Maywood). 2020;245(13):1073-86.
584 12. Chen Z, Han F, Du Y, Shi H, Zhou W. Hypoxic microenvironment in cancer: molecular
585 mechanisms and therapeutic interventions. Signal Transduct Target Ther. 2023;8(1):70.
586 13. Matic N, Pettersson L, Sellebjerg F, Lindberg L, Roberg K, Wiechec E. Prognostic value of hypoxia-
587 responsive gene expression profile in patients diagnosed with head and neck squamous cell carcinoma.
588 Transl Oncol. 2024;39:101841.
589 14. Li Y, Huang H, Jiang M, Yu N, Ye X, Huang Z, et al. Identification and validation of a hypoxia-
590 immune signature for overall survival prediction in lung adenocarcinoma. Front Genet. 2022;13:975279.
591 15. Rahal Z, El Darzi R, Moghaddam SJ, Cascone T, Kadara H. Tumour and microenvironment
592 crosstalk in NSCLC progression and response to therapy. Nat Rev Clin Oncol. 2025;22(7):463-82.
593 16. Shi R, Sun J, Zhou H, Hu T, Gao Z, Wang X, et al. Hypoxia within tumor microenvironment
594 characterizes distinct genomic patterns and aids molecular subtyping for guiding individualized
595 immunotherapy. Journal of Big Data. 2024;11(1):81.
596 17. Cerami E, Gao J, Dogrusoz U, Gross BE, Sumer SO, Aksoy BA, et al. The cBio cancer genomics
597 portal: an open platform for exploring multidimensional cancer genomics data. Cancer Discov.
598 2012;2(5):401-4.
599 18. Huang da W, Sherman BT, Lempicki RA. Bioinformatics enrichment tools: paths toward the
600 comprehensive functional analysis of large gene lists. Nucleic Acids Res. 2009;37(1):1-13.
601 19. Benjamini Y, Hochberg Y. Controlling the False Discovery Rate: A Practical and Powerful
602 Approach to Multiple Testing. Journal of the Royal Statistical Society: Series B (Methodological).
603 1995;57(1):289-300.
604 20. Szklarczyk D, Gable AL, Lyon D, Junge A, Wyder S, Huerta-Cepas J, et al. STRING v11: protein-
605 protein association networks with increased coverage, supporting functional discovery in genome-wide
606 experimental datasets. Nucleic Acids Res. 2019;47(D1):D607-D13.
607 21. Chin CH, Chen SH, Wu HH, Ho CW, Ko MT, Lin CY. cytoHubba: identifying hub objects and sub-
608 networks from complex interactome. BMC Syst Biol. 2014;8 Suppl 4(Suppl 4):S11.
609 22. Therneau T. A package for survival analysis in R. (95).
610 23. Friedman JH, Hastie T, Tibshirani R. Regularization Paths for Generalized Linear Models via
611 Coordinate Descent. Journal of Statistical Software. 2010;33(1):1 - 22.
612 24. Aguirre-Gamboa R, Gomez-Rueda H, Martinez-Ledesma E, Martinez-Torteya A, Chacolla-
613 Huaringa R, Rodriguez-Barrientos A, et al. SurvExpress: an online biomarker validation tool and database
614 for cancer gene expression data using survival analysis. PLoS One. 2013;8(9):e74250.
615 25. Zhao Y, Xing C, Deng Y, Ye C, Peng H. HIF-1alpha signaling: Essential roles in tumorigenesis and
616 implications in targeted therapies. Genes Dis. 2024;11(1):234-51.
617 26. Barnum KJ, O'Connell MJ. Cell cycle regulation by checkpoints. Methods Mol Biol. 2014;1170:29-
618 40.
619 27. Pedroza-Garcia JA, Xiang Y, De Veylder L. Cell cycle checkpoint control in response to DNA
620 damage by environmental stresses. Plant J. 2022;109(3):490-507.

621 28. Rankin BD, Rankin S. The MCM2-7 Complex: Roles beyond DNA Unwinding. Biology (Basel).
622 2024;13(4).
623 29. Bertoli C, Herlihy AE, Pennycook BR, Kriston-Vizi J, de Bruin RAM. Sustained E2F-Dependent
624 Transcription Is a Key Mechanism to Prevent Replication-Stress-Induced DNA Damage. Cell Rep.
625 2016;15(7):1412-22.
626 30. Zhang Y, Wen GM, Wu CA, Jing ZL, Li DZ, Liu GL, et al. PRKDC is a prognostic marker for poor
627 survival in gastric cancer patients and regulates DNA damage response. Pathol Res Pract.
628 2019;215(8):152509.
629 31. Klomp JE, Lee YS, Goodwin CM, Papke B, Klomp JA, Waters AM, et al. CHK1 protects oncogenic
630 KRAS-expressing cells from DNA damage and is a target for pancreatic cancer treatment. Cell Rep.
631 2021;37(9):110060.
632 32. Ooi AT, Gomperts BN. Molecular Pathways: Targeting Cellular Energy Metabolism in Cancer via
633 Inhibition of SLC2A1 and LDHA. Clin Cancer Res. 2015;21(11):2440-4.
634 33. Hanahan D, Weinberg RA. Hallmarks of cancer: the next generation. Cell. 2011;144(5):646-74.
635 34. Chen DS, Mellman I. Oncology meets immunology: the cancer-immunity cycle. Immunity.
636 2013;39(1):1-10.
637 35. Schreiber RD, Old LJ, Smyth MJ. Cancer immunoediting: integrating immunity's roles in cancer
638 suppression and promotion. Science. 2011;331(6024):1565-70.
639 36. Herbst RS, Morgensztern D, Boshoff C. The biology and management of non-small cell lung
640 cancer. Nature. 2018;553(7689):446-54.
641 37. Bandarra D, Biddlestone J, Mudie S, Muller HA, Rocha S. HIF-1alpha restricts NF-kappaB-
642 dependent gene expression to control innate immunity signals. Dis Model Mech. 2015;8(2):169-81.
643 38. Pang X, Xie R, Zhang Z, Liu Q, Wu S, Cui Y. Identification of SPP1 as an Extracellular Matrix
644 Signature for Metastatic Castration-Resistant Prostate Cancer. Front Oncol. 2019;9:924.
645 39. Napoli S, Scuderi C, Gattuso G, Bella VD, Candido S, Basile MS, et al. Functional Roles of Matrix
646 Metalloproteinases and Their Inhibitors in Melanoma. Cells. 2020;9(5).
647 40. Bhattacharyya S, Mote RD, Freimer JW, Tiwari M, Bansi Singh S, Arumugam S, et al. Cell-cell
648 adhesions in embryonic stem cells regulate the stability and transcriptional activity of beta-catenin. FEBS
649 Lett. 2022;596(13):1647-60.
650 41. French R, Pauklin S. Epigenetic regulation of cancer stem cell formation and maintenance. Int J
651 Cancer. 2021;148(12):2884-97.
652 42. Mirzaei S, Paskeh MDA, Entezari M, Mirmazloomi SR, Hassanpoor A, Aboutalebi M, et al. SOX2
653 function in cancers: Association with growth, invasion, stemness and therapy response. Biomed
654 Pharmacother. 2022;156:113860.
655 43. Baker SJ, Poulikakos PI, Irie HY, Parekh S, Reddy EP. CDK4: a master regulator of the cell cycle
656 and its role in cancer. Genes Cancer. 2022;13:21-45.
657 44. Choi SA, Moon YJ, Koh EJ, Phi JH, Lee JY, Kim KH, et al. Cyclin-Dependent Kinase Inhibitor 2A is a
658 Key Regulator of Cell Cycle Arrest and Senescence in Endothelial Colony-Forming Cells in Moyamoya
659 Disease. J Korean Neurosurg Soc. 2023;66(6):642-51.
660 45. Yarden RI, Brody LC. BRCA1 interacts with components of the histone deacetylase complex. Proc
661 Natl Acad Sci U S A. 1999;96(9):4983-8.
662 46. Bhaskara S. Histone deacetylases 1 and 2 regulate DNA replication and DNA repair: potential
663 targets for genome stability-mechanism-based therapeutics for a subset of cancers. Cell Cycle.
664 2015;14(12):1779-85.
665 47. Allen JR, Ge L, Huang Y, Brauer R, Parimon T, Cassel SL, et al. TIMP-1 Promotes the Immune
666 Response in Influenza-Induced Acute Lung Injury. Lung. 2018;196(6):737-43.
667 48. Elemam NM, Talaat IM, Maghazachi AA. CXCL10 Chemokine: A Critical Player in RNA and DNA
668 Viral Infections. Viruses. 2022;14(11).

49. Schultheiss C, Willscher E, Paschold L, Gottschick C, Klee B, Henkes SS, et al. The IL-1beta, IL-6, and TNF cytokine triad is associated with post-acute sequelae of COVID-19. Cell Rep Med. 2022;3(6):100663.
50. Zheng M, Ambesi A, McKeown-Longo PJ. Role of TLR4 Receptor Complex in the Regulation of the Innate Immune Response by Fibronectin. Cells. 2020;9(1).
51. Guerra-Espinosa C, Jimenez-Fernandez M, Sanchez-Madrid F, Serrador JM. ICAMs in Immunity, Intercellular Adhesion and Communication. Cells. 2024;13(4).
52. del Puerto-Nevado L, Rojo F, Zazo S, Carames C, Rubio G, Vega R, et al. Active angiogenesis in metastatic renal cell carcinoma predicts clinical benefit to sunitinib-based therapy. Br J Cancer. 2014;110(11):2700-7.
53. Angeli V, Hammad H, Staels B, Capron M, Lambrecht BN, Trottein F. Peroxisome proliferator-activated receptor gamma inhibits the migration of dendritic cells: consequences for the immune response. J Immunol. 2003;170(10):5295-301.
54. Guyon A. CXCL12 chemokine and its receptors as major players in the interactions between immune and nervous systems. Front Cell Neurosci. 2014;8:65.
55. Huang H, Wang Q, Ma L, Wu Y. ITGAM: A Pivotal Regulator in Macrophage Dynamics and Cardiac Function During Sepsis-Induced Cardiomyopathy. Cureus. 2024;16(4):e59342.
56. Li K, Quan L, Huang F, Li Y, Shen Z. ADAM12 promotes the resistance of lung adenocarcinoma cells to EGFR-TKI and regulates the immune microenvironment by activating PI3K/Akt/mTOR and RAS signaling pathways. Int Immunopharmacol. 2023;122:110580.
57. Ma G, Yang L, Dong J, Zhang L. CCNE1 Promotes Progression and is Associated with Poor Prognosis in Lung Adenocarcinoma. Curr Pharm Biotechnol. 2022;23(9):1168-78.
58. Cizkova M, Vacher S, Meseure D, Trassard M, Susini A, Mlcuchova D, et al. PIK3R1 underexpression is an independent prognostic marker in breast cancer. BMC Cancer. 2013;13:545.
59. Wei X, Chen L, Yang A, Lv Z, Xiong M, Shan C. ADRB2 is a potential protective gene in breast cancer by regulating tumor immune microenvironment. Transl Cancer Res. 2021;10(12):5280-94.
60. Zhang G, Chen Z, Wang Y, Huang A, Nie F, Gao L, et al. Up-regulated DSG2 promotes tumor growth and reduces immune infiltration in cervical cancer. Pathol Res Pract. 2024;262:155554.
61. Zhu W, Li GX, Chen HL, Liu XY. The role of eukaryotic translation initiation factor 6 in tumors. Oncol Lett. 2017;14(1):3-9.
62. Yang G, Dong K, Zhang Z, Zhang E, Liang B, Chen X, et al. EXO1 Plays a Carcinogenic Role in Hepatocellular Carcinoma and is related to the regulation of FOXP3. J Cancer. 2020;11(16):4917-32.
63. Liu Z, Huang S, Luo R, Shi X, Xiu M, Wang Y, et al. EXO1's pan-cancer roles: diagnostic, prognostic, and immunological analyses through bioinformatics. Discov Oncol. 2025;16(1):310.
64. Myo Min KK, Ffrench CB, McClure BJ, Ortiz M, Dorward EL, Samuel MS, et al. Desmoglein-2 as a cancer modulator: friend or foe? Front Oncol. 2023;13:1327478.
65. Sun L, Liu S, Wang X, Zheng X, Chen Y, Shen H. eIF6 promotes the malignant progression of human hepatocellular carcinoma via the mTOR signaling pathway. J Transl Med. 2021;19(1):216.
66. Garcia-Rodriguez N, Dominguez-Garcia I, Dominguez-Perez MDC, Huertas P. EXO1 and DNA2-mediated ssDNA gap expansion is essential for ATR activation and to maintain viability in BRCA1-deficient cells. Nucleic Acids Res. 2024;52(11):6376-91.

Supplementary Information

Supplementary Tables S1-S9

Supplementary Table S1. List of collected hypoxia related genes.

Supplementary Table S2. List of DEGs in TCGA LUAD.

Supplementary Table S3. List of DEGs in GSE18842.

Supplementary Table S4. List of hypoxia related DEGs in the both datasets.

Supplementary Table S5. Enriched pathways associated with the upregulated genes (FDR < 0.05).

Supplementary Table S6. Enriched pathways associated with the downregulated genes (FDR < 0.05).

Supplementary Table S7. Rank of the PPI network by Degree method.

Supplementary Table S8. Significant Genes Identified in Kaplan-Meier Survival Analysis.

Supplementary Table S9. Significant Genes Identified in Univariate regression Analysis.